

Article

Soil Moisture Profiles of Unsaturated Colluvial Slopes Susceptible to Rainfall-Induced Landslides

Paolo Paronuzzi, Marco Del Fabbro and Alberto Bolla * 

Polytechnic Department of Engineering and Architecture, University of Udine, 33100 Udine, Italy; paolo.paronuzzi@uniud.it (P.P.); marco.delfabbro@uniud.it (M.D.F.)

* Correspondence: alberto.bolla@uniud.it; Tel.: +39-0432-558738

Abstract: In this work, we describe soil moisture profiles related to typical colluvial slopes that were involved in rainfall-induced shallow failures occurring in alpine and pre-alpine areas of the Friuli Venezia Giulia Region (NE Italy). The trend of the volumetric water content (θ_w) showed a general increase from the ground surface to the bottom soil layer, with two or three marked moisture peaks. The saturation degree (S) varied from 65–70% (topsoil horizon) to nearly saturated basal colluvium (S = 95–100%). Soil moisture data demonstrates that, for a very humid climate, colluvial covers are often close to the saturation condition for most of the year. The calculated suction profiles indicated that maximum values ranging from 40 to 55 kPa often occur in the slope surficial soil (depth < 0.2–0.5 m). This negative pore-water pressure greatly decreases after a heavy rainfall event because of the infiltration process. Complete saturation of colluvial cover in the alpine and pre-alpine regions generally requires rainfall exceeding 150–200 mm for a 24-h storm duration. This results in a recurrence time of $T_r \cong 5$ –10 years for critical rainfall episodes involving colluvial slopes in the Friuli Venezia Giulia Region. The case histories analyzed demonstrate the importance of performing a detailed lithostratigraphic analysis of the colluvial deposit in order to properly define the suction measurement points, which there should be more of than the three-point determinations usually reported in the literature (for example, $z = 0.5, 1.0$ and 1.5 m).

Keywords: colluvial slope; shallow landslide; unsaturated soil; moisture profile; volumetric water content; heavy rainfall



Citation: Paronuzzi, P.; Del Fabbro, M.; Bolla, A. Soil Moisture Profiles of Unsaturated Colluvial Slopes Susceptible to Rainfall-Induced Landslides. *Geosciences* **2022**, *12*, 6. <https://doi.org/10.3390/geosciences12010006>

Academic Editors: Samuele Segoni and Jesus Martinez-Frias

Received: 25 November 2021

Accepted: 22 December 2021

Published: 24 December 2021

Publisher's Note: MDPI stays neutral with regard to jurisdictional claims in published maps and institutional affiliations.



Copyright: © 2021 by the authors. Licensee MDPI, Basel, Switzerland. This article is an open access article distributed under the terms and conditions of the Creative Commons Attribution (CC BY) license (<https://creativecommons.org/licenses/by/4.0/>).

1. Introduction

Colluvial slopes in mountain areas of the European Alps are often affected by shallow failures triggered by storm events. Most of them are referred to as soil slips [1,2] or slide-debris flows, according to the landslide terminology proposed by Varnes [3] and further reviewed by Cruden and Varnes [4]. In order to adequately simulate the infiltration process and to perform the related stability analyses of these shallow landslides, the assumption of realistic initial hydrological conditions [5–7], i.e., adequate knowledge of the in situ volumetric water content (θ_w) and the determination of the related suction values (u_a – u_w), are required. In fact, the assumption of a proper degree of saturation (S) of the colluvial cover is of key importance in order to set up an infiltration modeling of the slope, for both approximated and rigorous approaches. These hydrologic models, which are of various complexity, can provide useful information as to whether the investigated colluvial slope can reach the saturation condition as a result of heavy rainfall, thus favoring the occurrence of an ephemeral subsurface groundwater table [8]. The latter represents a major cause of the critical stability condition of a slope, possibly triggering its failure [9,10]. This is especially true for colluvial slopes susceptible to shallow failures involving 2–3 m-thick debris covers. Over the past few decades, many researchers have focused on the importance of adopting a proper shear strength criterion for unsaturated materials ([11] and references therein), and remarkable improvements have been made in evaluating the strength contribution due to suction, starting from the basic approach formulated for the first time by Fredlund

et al. [12], which assumed the angle of friction associated with the soil suction as a constant soil parameter, up to traditional stress-dependent formulations [8,13] or newly proposed approaches that consider a thermodynamic expression for Bishop's effective stress [14].

Even recently, several case studies have stressed the importance of assessing the initial soil suction within the slope (i.e., before critical rainfall) in order to properly investigate possible variations in the stability condition of the slope caused by various rainfall patterns [10,15–18]. Consequently, the simulation of the infiltration process, as well as the subsequent analysis of the slope stability condition, require the adoption of a sufficiently detailed stratigraphic schematization along with the estimation of the initial condition of saturation of the slope before the start of intense precipitation. Many examples of infiltration and saturation models used to analyze heavy rainfall-induced landslides have been presented [19–25], but this approach requires an in-depth knowledge of the hydrological properties of the soils. In the literature, most attention has been paid to the reconstruction of the soil–water characteristic curve (SWCC) of soil involved in the slope infiltration process [26]. As a result, most geotechnical investigations on colluvial or “residual” slopes are aimed at determining the water content and/or the suction stress within the soils forming the colluvial deposit. Different measuring techniques and devices were employed to determine both the water content and the matric suction of soils. The diverse devices adopted and testing procedures have both strengths and limitations and were used variously by researchers in relation to the specific case study in order to maximize the validity of the measurement results.

Suction measurements on unsaturated colluvial slopes were carried out in situ by means of tensiometers that were installed in boreholes [27,28] or on exposed surfaces of the colluvial deposit [29]. Suction values were recorded at a depth (z) of 0.5, 1.0 and 1.5 m [27] or 0.3, 0.6 and 1.3 m [29] because of the prevailing occurrence of shallow failures ($z \leq 1.5$ m). Filter paper tests [30] and heat dissipation sensors [31] were also used to measure the suction stress in situ. In addition, suction determinations were also carried out in the laboratory on representative soil specimens using the pressure plate method [30,32,33]. These in situ suction measurements often showed a marked curvilinear trend with suction decreasing greatly from the surficial soil to the deeper colluvium ($z = 1.5$ m), where a near-saturated condition predominates and suction approximates to zero [27]. Otherwise, the natural water content of the soil has frequently been determined in situ using neutron probes [34,35] and time domain reflectometers (TDRs) that were installed in boreholes or trial pits at variable depths [31,36–38], whereas moisture sensors have been used more rarely in laboratory experiments [39–41].

Soil moisture profiles and the saturation process of colluvial covers are influenced by several factors, including: (i) the stratification of the slope deposits, (ii) the previous degree of saturation, and (iii) the hydraulic conductivity (K) of the different soil types and sediments. When considering a typical cross section of a natural colluvial slope, the variation of the volumetric water content (θ_w) within the shallow soil horizons is strongly affected by pedogenetic features including macro-porosity, root development, vertical fissures and clay illuviation. Sedimentary processes and specific stratigraphical features, which are related to the geological evolution of the slope, can determine some complex stratification conditions with abrupt changes in grain size and permeability properties of soils. Sudden or even unexpected moisture variations in the slope profile can occur at greater depth as a consequence of marked lithostratigraphical changes (stratified colluvial deposits) due to distinct deposits mobilized by previous landslides or earth flow processes. This is a typical situation for channelized colluvial slopes when previously failed landslide deposits are lodged within a “landslide gully” and are periodically remobilized during specific instability episodes caused by heavy or prolonged rainfall. These particularly unstable channelized slopes are characterized by thicker colluvial deposits (5–10 m, very often) caused by the superimposition of distinct preexisting landslide deposits, highlighting a recurrent instability condition of the slope.

However, the trend of saturation at depth and the stratigraphic sequence of colluvial covers in the Alpine area are not yet understood in sufficient detail. Although several infiltration models for unsaturated colluvial slopes have been proposed in the literature, subsurface soil moisture profiles and saturation degree determinations have been rarely reported, particularly in relation to the specific stratigraphic sequence of the colluvial deposit [28,31,42]. This difficulty in obtaining adequate hydrological parameters for the failure-involved slope materials reduces the use of unsaturated analysis in current slope engineering practice [43]. This may be explained by the objective difficulties related to the in situ measurement of the degree of saturation, along with the common practice of preferring localized borehole investigations rather than direct field observations obtained from the analysis of wider stratigraphic sections outcropping on the slope face in correspondence with landslide scarps or exploratory trenches.

All the aforementioned issues highlight the general need for a better understanding of the soil moisture condition within the surficial layers of colluvial slopes. Toward this aim, detailed stratigraphical analyses and moisture determinations related to unsaturated colluvial slopes occurring in mountain areas of the Friuli Venezia Giulia Region (northeastern Italy) will be presented in this work (Figure 1). Extensive field investigations and laboratory tests were carried out in order to provide useful insights into the lithostratigraphic features and moisture conditions of colluvial deposits involved in rainwater infiltration processes that are responsible for soil slope failures. Moisture profiles were repeatedly measured on alpine slopes that were involved in shallow landslides of both the soil slip and channelized slide-debris flow types. Soil moisture profiles were determined by means of field sampling that was carried out on landslide scarps. Moisture determinations were repeated during the dry and wet seasons in order to analyze the influence of climate and weathering on the degree of saturation of the slope. Laboratory tensiometer determination of the soil suction allowed us to evaluate the soil–water characteristic curve of the colluvium material and to calculate the suction profiles. The main goal of this research was to stress the importance of site-specific soil moisture data representing a basic input parameter to carry out subsequent coupled infiltration-stability analyses of unsaturated colluvial slopes that are aimed at investigating the critical conditions at failure.

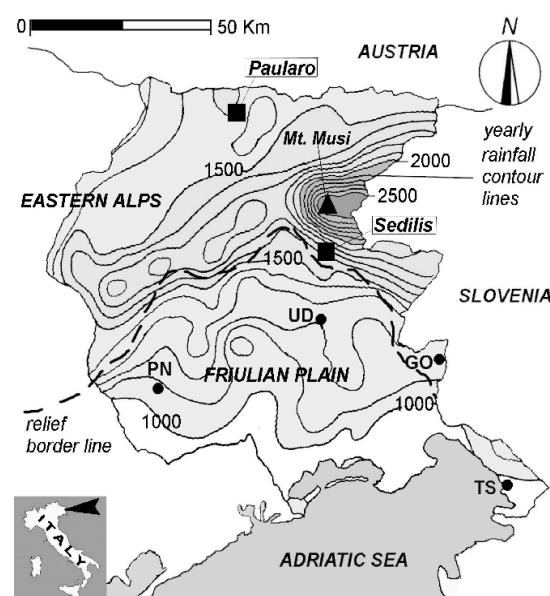


Figure 1. Map of the Friuli Venezia Giulia Region showing the yearly rainfall total data and the location of the studied case histories.

2. Alpine Climate and Rainfall Data

From a geographical point of view, the Friuli Venezia Giulia Region represents the eastern end of the Italian Alps. This mountain area, known as the Friulian Alps, is a part

of the alpine chain of the South Eastern Alps and borders to the north with the Austrian Alps and to the east with the Dinaric Alps forming the alpine relief of the adjacent state of Slovenia (Figure 1). The pre-alpine belt is bounded to the south by an alluvial plain, namely the Friulian Plain, which represents the easternmost part of the great alluvial plain related to the River Pò system. This particular geomorphological conformation causes an abrupt and sharp relief border belt, which develops where the mountain area meets the alluvial plain, so that the main climatical characteristics of the two regions are very different. The Friulian plain has a typical Mediterranean climate with a marked dry summer season and yearly rainfall ranging from 800 mm (coast) to 1300–1400 mm (upper plain and hills of the pre-Alps). The mountain area of the Friuli Venezia Giulia Region is characterized by a wetter and rainier climate, with average yearly rainfall always greater than 1500 mm and which typically increases northward and eastward in the pre-alpine area, where a marked peak of 2500 mm of yearly rainfall occurs in correspondence with the Mt. Musi relief (Figure 1).

The mountain area of the Friuli Venezia Giulia Region is also characterized by heavy rainstorms frequently occurring during the wet season (September–November) or during the spring period (May–June). As a rule, major storm episodes come from northwestern Italy because of the general eastward motion of the atmospheric perturbations forming in the Atlantic area. In these circumstances, 24-h rainfall totals greater than 150 mm are often recorded (Figure 2), but historical time records indicate that values greater than 200 mm are not uncommon (recurrence time: $Tr = 20\text{--}30$ years). Rainfall height peaks are considerably higher than the mean value of 125 mm calculated for the maximum yearly value (MYV) for a 24-h rain duration.

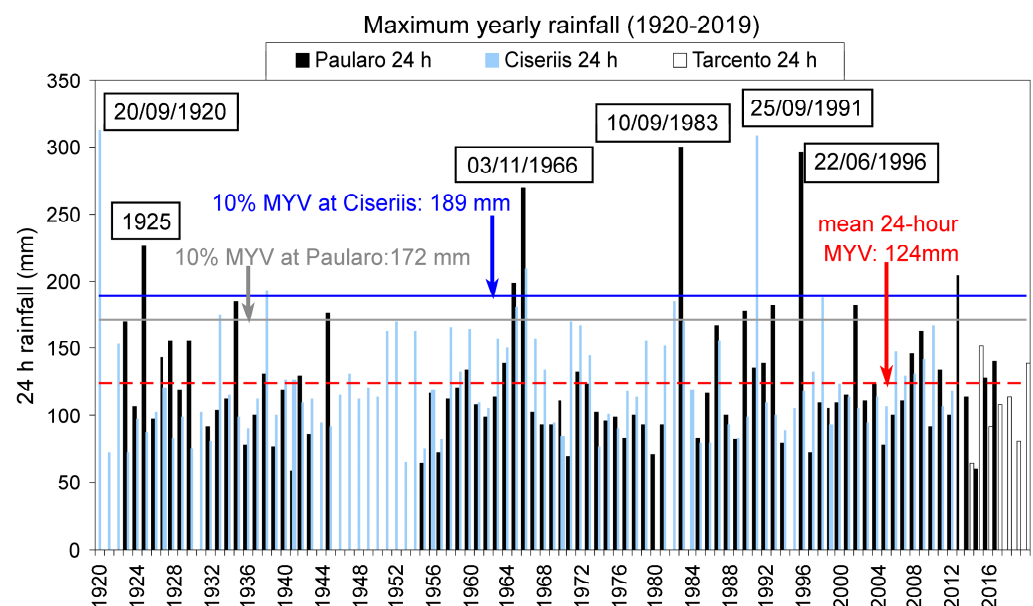


Figure 2. Maximum yearly 24 h rainfall totals that were recorded at the gauge stations of Paularo (alpine area), Ciseriis and Tarcento (pre-alpine area) during the 1920–2019 period.

The graph in Figure 2 also reports the maximum yearly values that were recorded during the period 1920–2019 in the alpine area (Paularo, Carnic Alps: mean yearly rainfall of 1719 mm) and pre-alpine area (Ciseriis and Tarcento, Julian Pre-Alps: mean yearly rainfall of 1886 mm). Since the rainfall gauge station of Ciseriis has not been in use since 2012, rainfall data for the past decade has been included in the graph in Figure 2, taking into consideration the nearby gauge station of Tarcento (about 1.5 km away from Ciseriis). The time record of the rainfall sequence shows these localities were hit by five severe storm events characterized by rainfall totals above 250 mm, and in some cases exceeding the value of 300 mm for precipitation falling over 24 h. The same histogram also points out the increasing frequency of these critical episodes since 1960, with several severe events

occurring over the past ten-year period of the century. Nonetheless, it must also be noted that, for the alpine and pre-alpine areas that were studied, the rainwater which has fallen over the past decade is characterized by lower intensity peaks when compared with 24-h rainfall occurring in the last 20 years of the past century (Figure 2).

As a result of intense precipitation in the mountain basins of the Friuli Venezia Giulia Region, many slope failures of variable size and/or catastrophic floods in the bottom valleys have occurred in the past. These critical events with heavy rainfall-induced disasters have increased since 1990 [44,45]. Many catastrophic episodes have occurred in distinct alpine basins, provoking extensive damage to human activities: 4 November 1966, 11 September 1983, 23–24 September 1990, 27 September 1991, 21–22 June 1996, 5 and 12 September 1998, 18 October 2000, 29 August 2003, 31 October–1 November 2004, 26–27 May 2007, 4 September 2009, 17–19 January 2014, 30 January–5 February 2014, 26–28 April 2017, 26–30 October 2018.

3. Colluvial Slopes of the Friuli Venezia Giulia Region

Soil slopes formed by a colluvial cover are widespread within the mountain basins of the Friuli Venezia Giulia Region. Their frequency is determined by the large extension of sedimentary rocks among which limestones, dolomitic rocks and terrigenous clastic sequences, including sandstones, siltstones, shales and marls, predominate. The alternating sandstone–marl sequence that characterizes many geological units related to Flysch sedimentary sequences of different ages, ranging from the Carboniferous (Palaeozoic Flysch of the Carnic Alps) to the Eocene (Flysch of Friuli, outcropping in the fore-alpine belt), is particularly prone to the formation of colluvial covers. The predominantly silty–marly nature of these sedimentary sequences makes this bedrock an excellent parent material for the generation of colluvial covers on gentle soil slopes. The colluvium deposits typically have a mean thickness of 1–3 m (Figure 3), but the cover can increase up to 5–10 m in some cases related to highly active slopes which are characterized by recurrent instability processes and/or channelized landslides. The formation of colluvial covers on the slopes of the mountain area of the Friuli Venezia Giulia Region is favored by the very humid and rainy climate (Figure 1). The considerable amount of yearly rainfall associated with the frequency of severe storms induces the repeated mobilization of surficial material which tends to increase the colluvium thickness at the toe of the slope or in low-tilted zones of the slope.

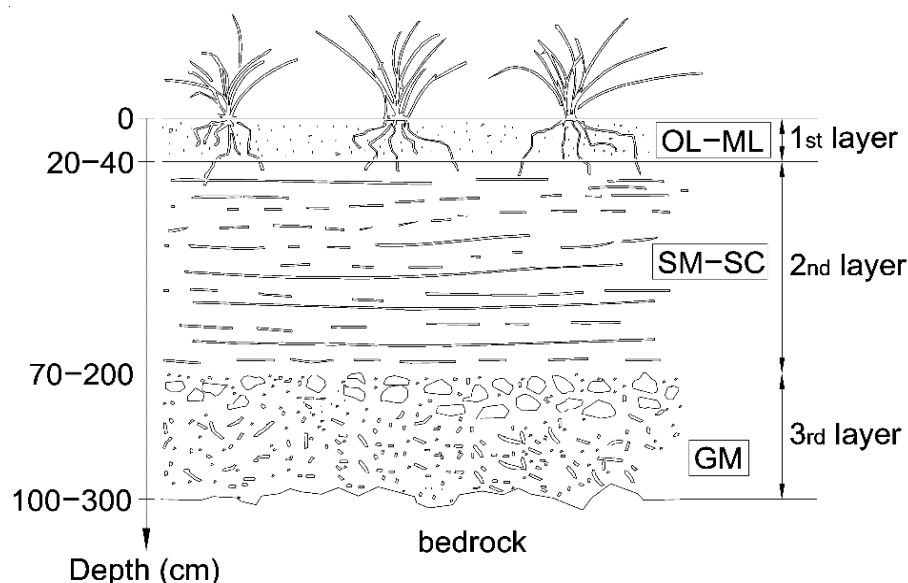


Figure 3. Typical stratigraphical section of colluvial slopes in mountain areas of the Friuli Venezia Giulia Region. This moderately thick surface stratigraphy is typical of terraced alluvial fans that are located at the valley bottoms, near the current river plains (i.e., thalweg).

Sliding, mass transport and material fluidization are the main geomorphological processes controlling the stratigraphy of the colluvial cover, thus determining the total thickness of the colluvial deposit and the occurrence of internal stratifications. Several field observations, which were performed by the authors on alpine colluvial slopes forming terraced belts, demonstrate a typical three-layer stratigraphy, which can be summarized as follows (Figure 3):

- 1st layer—A brown horizon of a surficial soil with a thickness of 20–40 cm mainly characterized by organic silts and clays (OL) and/or inorganic silts and very fine sands (ML);
- 2nd layer—colluvial stratum of an olive brown color made up of prevailing silty sands (SM) and clayey sands (SC) with a thickness varying from 50–200 cm, in most cases;
- 3rd layer—basal colluvial stratum of a yellowish brown or reddish brown color with a thickness of 30–100 cm made up of silty gravel with sand (GM) with abundant pebbles and angular rock fragments derived from the local bedrock. In many cases, this basal layer also includes a considerable amount of clay that is caused by the weathering of the underlying bedrock or is the result of pedogenetic processes involving the upper layers of the rock mass (illuvial clay).

The sedimentary bedrock that underlies the colluvial cover is typically weathered, often exhibiting diffused fracturing and including interbeds or seams of highly weathered claystone or marls. The second and third layers represent the actual “colluvium”, and the term “residual” should be avoided for these materials because the *in situ* weathering in alpine areas is a secondary process when compared with slope failures and creep phenomena.

As a rule, the colluvial sediments are very poorly sorted and the coarser fraction (gravel and sand) tends to equalize the finer fraction (silt and clay). Sand and clay contents are often influenced by the lithology of the underlying bedrock (limestone, sandstone, siltstone or marl). In some circumstances, the material deriving from loess deposits can greatly increase the sandy fraction. Due to the remobilization of older loess cover, this contribution is of key importance for the upper terraces of alpine valley slopes, where Late Pleistocene periglacial processes occurred. On the other hand, the clay content included in the colluvial deposits can be highly variable. Greater amounts of clay are related to the occurrence of shales or marly interbeds in the bedrock, especially if this is a fine-structured Flysch, i.e., thin stratification with shales alternated with siltstones or marls. Commonly, fine fractions are characterized by a low-medium plasticity, according to the prevalence of inactive or low-active clay minerals such as illite/muscovite, chlorite, kaolinite and interstratified clay minerals (illite/smectite). Fines also have considerable amounts of quartz, whenever the calcite content depends on the weathering degree of the colluvial cover and tends to decrease considerably for heavily weathered materials.

4. Studied Case Histories

In order to achieve a deeper knowledge on the soil stratigraphy and moisture conditions of unsaturated colluvial slopes susceptible to rainfall-induced landslides, a detailed engineering–geological survey was carried out in the field. Two basically different types of colluvial slope failures were examined, referring to both alpine terraced slopes and pre-alpine channelized colluvial deposits (Figures 4 and 5). The case histories studied are among the largest slope instability events involving colluvial deposits that have occurred in the past 30–40 years in the Friuli Venezia Giulia Region and were caused by rainstorms characterized by some of the highest values of rainfall intensity measured in the past 50 years (Figure 2). The large amount of data that were collected on these two case studies are of great interest to better understand moisture conditions of unsaturated colluvial slopes involved in rainfall-induced failures.

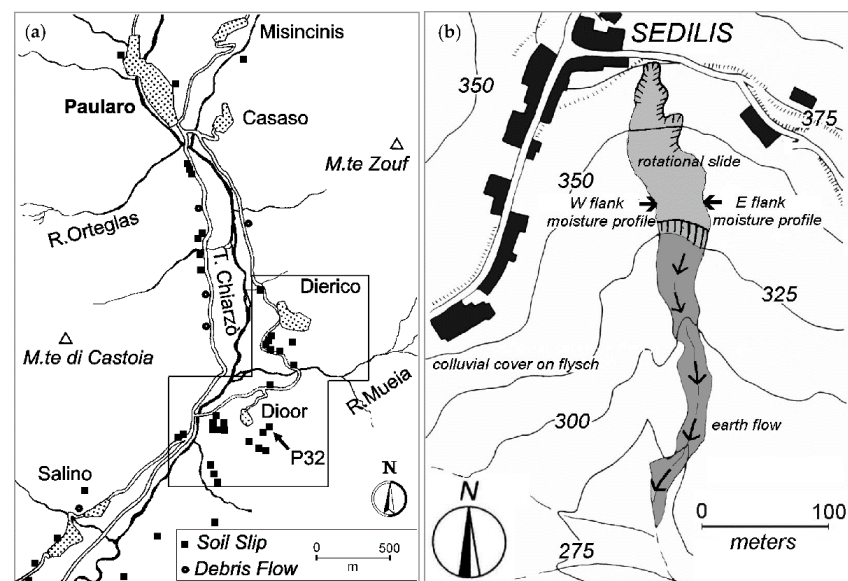


Figure 4. (a) Planimetric sketch of the shallow landslides that occurred on 22 June 1996 in the Chiarsò River valley. The location of the investigated soil slip (P32) is highlighted. (b) Planimetric sketch of the Sedilis landslide showing the channelized slide-earth flow that occurred on 14 September 1998. Sampling points on the lateral scarps are indicated by thick black arrows.



Figure 5. (a) Shallow rainfall-induced landslide which occurred on 22 June 1996 on a terraced slope along the Chiarsò River valley. (b) Upper part of the Sedilis slide-debris flow that occurred on 14 September 1998 and involved a preexisting dormant landslide-gully.

The first case history is associated with several shallow landslides (more than 40), referred to as soil slips or slide-debris flows, which were triggered by a heavy rainstorm that hit the Chiarsò River valley on 22 June 1996 (24-h rainfall of 295.8 mm; Figure 2), to the south of the village of Paularo (Figures 1 and 4a). During this event, a maximum peak of hourly rainfall intensity of 90 mm/h was recorded at 10 a.m. (GMT + 1) on 22 June by the rainfall gauge station of Paularo. During or soon after this maximum rainfall intensity, several shallow failures occurred on the terraced grass-cultivated slopes of the valley [46] (Figure 4a). Most of the slides generated some scarps at their crowns, immediately below the near-horizontal surface of the terraces (Figure 5a). Colluvial covers with thin deposits overlying the Triassic sedimentary bedrock characterize the terraces located at higher elevations compared with the valley bottom floor. The parent-material pertains to a complex sequence that includes the alternation of cm- to dm-thick limestone and marls (“Werfen” Formation).

The second case history considers a complex channelized slide-earth flow involving a thick colluvial cover resting on a gentle slope formed by alternating shales and sandstones of the Eocene Flysch (“Marne e Arenarie di Savorgnano” Formation) in the pre-alpine area of the Friuli Venezia Giulia Region (Figure 1). This slide took place near the village of Sedilis (Figures 4b and 5b), following a very humid period in the autumn of 1998 that culminated in two consecutive severe storms on 5 September (24-h precipitation of 181.6 mm) and 12 September (24-h precipitation of 188.0 mm). During the first heavy rainfall event which occurred on 5 September 1998, a maximum intensity value of 60 mm/h was recorded at the nearby Ciseriis gauge station (Figure 6).

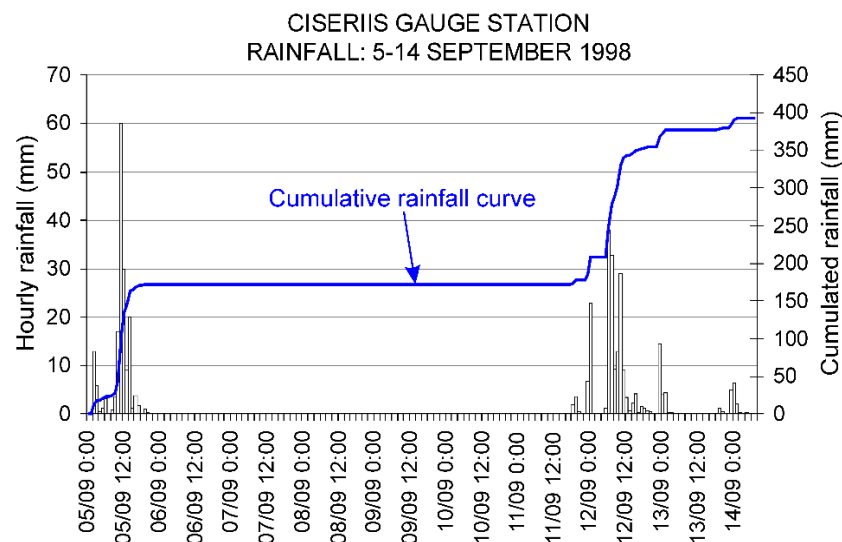


Figure 6. Cumulative rainfall and hourly rainfall over a 9-day period that preceded the Sedilis landslide which occurred on 14 September 1998.

Two days after the second storm, at 7.00 a.m. (GMT+1) on 14 September 1998, a sequence of rotational slides started at the top of the slope (Figure 5b), producing a channelized earth flow that propagated downward involving a little stream located further down the slope. At the end of the propagation of the fluidized colluvial material, the slide assumed the final shape of a very long (400 m) and narrow (20–30 m, on average) strip of mobilized terrain (Figure 4b). The total volume of the failed mass was estimated to be approximately 40,000 m³, and the depth of the failure surface was assumed to be from 2–3 m to 7–8 m below the ground surface. Two different stages of evolution were clearly recognized for the Sedilis landslide: a first rotational slope failure and a subsequent fluidization of the colluvial cover that determined the flow propagation of the collapsed mass.

These briefly summarized case histories relating to shallow failures of colluvial slopes have been the subject of a detailed morphological and lithostratigraphical analysis on the

field, and several soil samples were taken for the grain size and moisture characterization. Unlike stratigraphical reconstructions based on the correlation with single points of investigation (e.g., boreholes), the analysis of a stratigraphic section exposed along a scarp allows for the identification of the different stratified layers forming the colluvial deposit in detail, along with their variations in both vertical and horizontal directions. These field observations can be acquired from landslide scarps that were formed at the crown or at the lateral boundaries of previous slope failures. In this circumstance, field data is of key importance if it is acquired soon after slope failure on freshly exposed surfaces, prior to the possible drying out of the colluvial materials and/or subsequent covering due to small shallow debris sliding. The stratigraphic analysis of the exposed failure scarps also helps in defining a proper sampling procedure of the colluvial materials, considering the specific stratigraphy of the deposit. This means that the soil samples can be collected at a variable depth from the different layers that actually form the colluvial deposit, without referring to pre-established fixed sampling intervals (for example, at 0.5, 1.0 and 1.5 m depth) that are frequently chosen on the basis of borehole investigations. As a result, the detailed stratigraphic analysis of the colluvial deposit and the specific soil sampling represent a valuable procedure in obtaining basic information required to properly set up the hydrologic and geotechnical models of the slope. This procedure has been adopted in the case histories investigated in the present work and is based on some distinct field activities, as follows:

- Geomorphologic survey of the lateral and/or crown scarps of the colluvial slope failures, with selection of the most important outcrops from stratigraphic and hydrologic points of view;
- Stratigraphic analysis of the colluvial deposit, with identification and codification of the different stratigraphic units. The outcrops were preliminarily cleaned using trowels and brushes, removing possible debris cover and pointing out the stratigraphic boundaries among the colluvial layers as well as the basal contact between the colluvial deposit and the underlying bedrock;
- Soil sampling at selected locations using steel cylindrical samplers with a cutting edge. The soil samples were sealed and rapidly brought to the geotechnical laboratory (within 3–6 h) for the determination of the weight, natural water content and degree of saturation.

The soil samples collected by means of the sample cutters were affected by a minimal disturbance mainly related to the side friction between the cutter walls and the coarser particles included in the soil mixture (cobbles and angular rock fragments). During the sampling operation, an attempt was made to minimize the contact between the cutter and the rock fragments. On the one hand, the increase in the volume of the sampler reduces the error associated with the volumetric determination, and consequently increases the accuracy of the saturation degree determinations; but on the other hand, it increases the probability of contact with the coarser particles and, therefore, the extent of the disturbance. The objective difficulty of obtaining undisturbed samples from heterogeneous materials with a relevant coarse fraction (cobbles and blocks), as commonly included in colluvial covers, must also be kept in mind. In these circumstances, a certain level of disturbance during the soil sampling must be considered unavoidable. However, the stratigraphic analysis and the preliminary preparation of the slope outcrop allowed for the identification of the most suitable sampling points, thus reducing the disturbance effect induced by the coarser rock fragments. In the case of problematic and/or disturbed sampling, the latter was repeated in another point of the scarp, but in the same stratigraphic position. The main aim of this sampling procedure was to obtain a detailed stratigraphic section associated with a vertical moisture profile to provide realistic values of the degree of saturation of the colluvial slope. To achieve this scope, several samples were collected and the sampling procedure was repeated in different seasons.

The stratigraphic analysis that was performed on the colluvial terrace exposed at the crown scarp of the Dior slide allowed us to identify eight distinct stratigraphic units (from C1 to C8 in Figure 7a). The colluvial deposit was subdivided into three main

layers (Figure 7b): the first layer (C1) was a surficial, 40 cm-thick organic horizon with abundant root development; the second layer (C2–C6) was an olive brown, 250 cm-thick soil prevailingly made up of a sand–silt–clay mixture; the third layer (C7–C8) was a yellowish brown, 150 cm-thick soil mixture that also included coarser particles (cobbles and rock pieces), especially in the upper unit (C7).

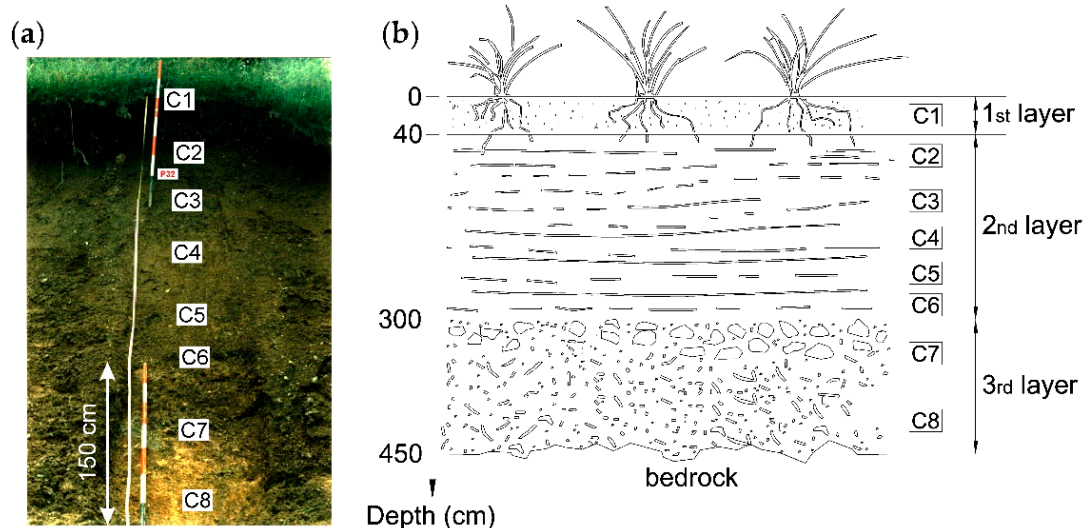


Figure 7. (a) Stratigraphical section exposed at the crown scarp of landslide P32 (Dioor slide); and (b) its schematization. The stratigraphical location of the soil samples (C1–C8) is also shown.

The colluvial cover involved in the Sedilis slide-debris flow had marked differences compared with the terraced colluvial deposit of Dioor, including the type of parent material (Eocene Flysch vs. Triassic marly limestone sequence), the grain size composition (higher finer fractions vs. higher coarser fractions) and the geomorphologic context (channelized vs. terraced slope). In addition, the total thickness of the Sedilis colluvial deposit (7–8 m) was greater than that of the Dioor slide (4.0–4.5 m).

According to the grain size investigations (Figure 8), gravel and pebbles represented a considerable part of the soil particles and their average amount reached one-third of the total mass (34%), for both the investigated cases (Tables 1 and 2). The second important grain size fraction was the silt fraction, with percentages ranging from 22–35%, in most cases (Tables 1 and 2). Sand and clay fractions were more variable.

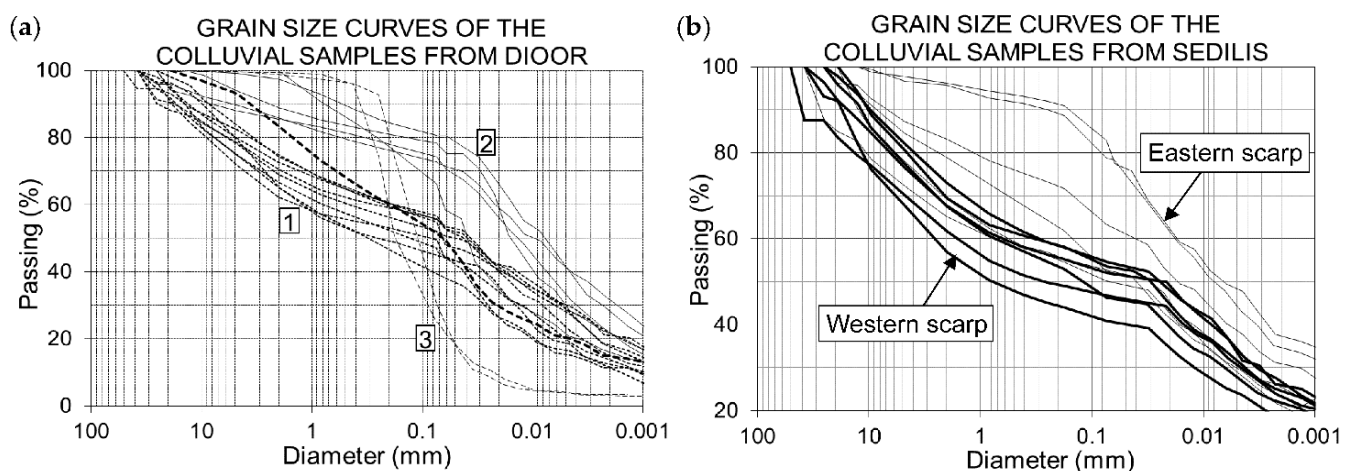


Figure 8. Grain size distribution curves of the colluvial materials sampled from: (a) the Dioor slide; and (b) the eastern (EF) and western (WF) scarps of the Sedilis slide. Note the different groups of the sampled materials.

Table 1. Grain size fractions of colluvial materials that were sampled at variable depths from the Dioor slide (landslide P32).

Sample	Depth (m)	Gravel (%)	Sand (%)	Silt (%)	Clay (%)	Silt/Clay
C1	0.15	21.2	33.5	35.1	10.3	3.4
C2	0.45	31.8	22.2	30.8	15.2	2.0
C3	1.00	44.8	21.3	22.2	11.7	1.9
C4	1.60	37.7	24.8	24.9	12.7	2.0
C5	2.30	31.3	23.1	31.4	14.2	2.2
C6	2.60	32.9	24.4	27.8	14.9	1.9
C7	3.00	52.4	28.6	13.5	5.6	2.4
C8	3.45	19.1	30.9	39.0	11.1	3.5
mean		33.9	26.1	28.1	12.0	2.3

Table 2. Grain size composition of the colluvial soils that were sampled at variable depths from the Sedilis landslide (western lateral scarp).

Sample	Depth (m)	Gravel (%)	Sand (%)	Silt (%)	Clay (%)	Silt/Clay
C10	2.65	32.5	21.7	24.1	21.7	1.1
C8	3.65	30.6	16.4	28.5	24.6	1.2
C6	4.65	43.0	16.7	22.1	18.2	1.2
C4	5.55	27.1	19.1	28.0	25.8	1.1
C2	6.30	38.3	15.7	22.8	23.2	1.0
C0	7.10	32.3	16.2	25.0	26.5	0.9
mean		34.0	17.6	25.1	23.4	1.1

On the whole, sand percentages ranged from 16–34%, with mean values of 26% for the Dioor slide (Table 1) and 18% for the Sedilis slide (Table 2). The opposite occurred for the clay contents, which overall varied from 10–26%, but were higher, on average, for the Sedilis slide (23%) compared with the Dioor slide (12%). On the basis of this sedimentological data, the analyzed colluvial deposits can be defined as poorly sorted silty–loamy materials with 40–48% of a fine matrix, on average, even reaching in some cases a prevailing content of 54%. However, it was possible to differentiate a finer colluvium with a silt/clay ratio close to 1.0 (0.9–1.2) (Table 2) from a silty colluvial deposit with a greater silt/clay ratio (1.9–3.5) (Table 1).

5. Moisture Profiles

Moisture profiles were measured at different times on typical colluvial slopes, both in alpine (landslide P32 at Dioor) and pre-alpine (Sedilis landslide) areas. Soil sampling was performed at 10–15 cm depth intervals on shallower cover (Dioor) and at 40–60 cm depth intervals on thicker colluvial deposits (Sedilis). Sampling was carried out on landslide failure scarps after section refreshing and removal of the drier surface material. Sampled soil profiles refer to both the upper scarp of the Dioor slope failure and the lateral flanks of the Sedilis landslide (Figure 4). The results of the analyzed soil profiles obtained for different climatic zones, i.e., alpine and pre-alpine environments, were then compared to identify the moisture conditions and the variations in the saturation degree (S) within the colluvial cover caused by seasonal changes.

Two moisture profiles measured on the colluvial scarp of landslide P32 at Dioor are reported in Figure 9, where symbols indicate the sampling points. Samples were taken during both the wet (9 December 1997) and dry (24 June 1998) seasons. The saturation degree varied from 70–75% for the top layer or soil horizon to 98–100% for the near-saturated basal colluvium.

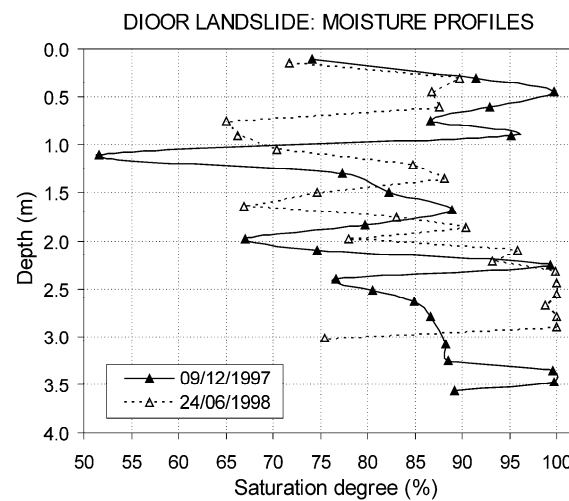


Figure 9. Variations of the saturation degree within the colluvial cover at Dioor (landslide P32).

The saturation curve recorded during the winter period exhibits a marked minimum value of $S = 52\%$ at a depth of 110–120 cm. Mean values of the saturation degree, calculated for all the profiles, are close to 85% and the yearly variation is negligible (85–87%), according to the acquired measurements (Figure 10). This moisture data confirms that the basal colluvium in alpine slopes is in near-saturated conditions during various months of the year, particularly during the rainy seasons (September–November and May). The saturation curves are highly irregular, with many moisture peaks that are separated by marked minimum values. Moisture variations at depth are often abrupt and the location of positive and negative peaks does not remain the same during the year (Figure 9).

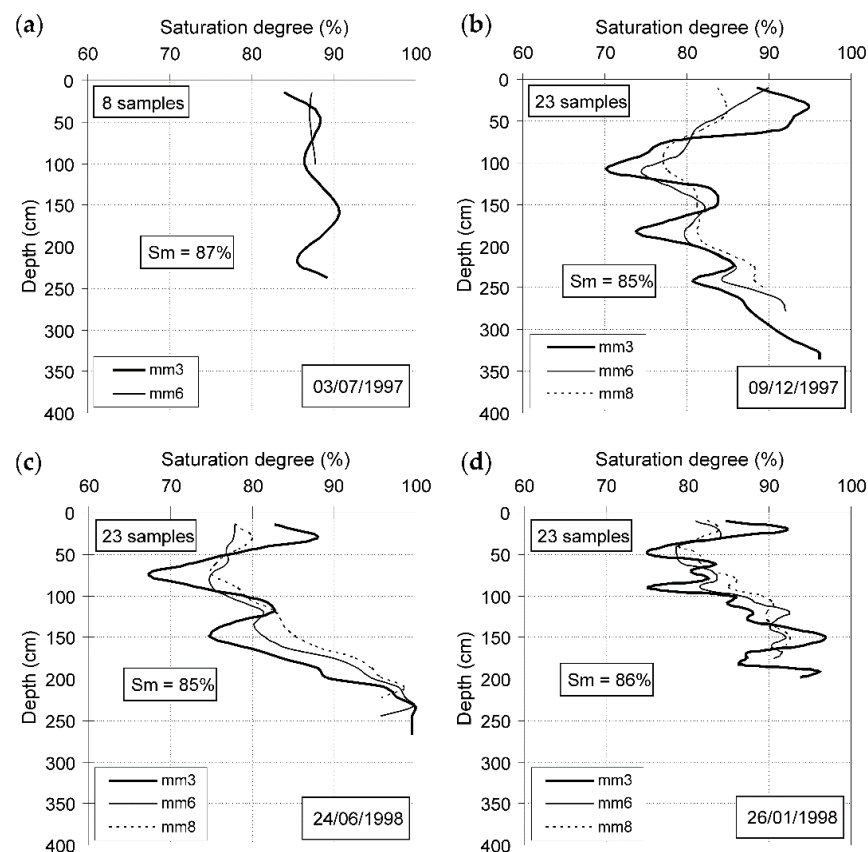


Figure 10. Trends of various mobile means (mm = 3, 6 and 8) of the saturation degree measured in summer (a,c) and winter (b,d) seasons at Dioor (landslide P32).

To better display this general trend, four saturation curves that are drawn in terms of different mobile means ($\text{mm} = 3, 6$ and 8) are shown in Figure 10. The moisture profiles obtained from multiple soil sampling show that the general trend of the various profiles is more significant than the single values of the saturation degree at one point, these being local measurements possibly affected by some errors due to specific sampling difficulties and extent of disturbance. In addition, the same field sampling and laboratory testing procedures were repeated for all the collected soil samples, thus ensuring comparable errors. For these reasons, the possible sample disturbance did not affect the general significance of the moisture profiles and average degrees of saturation, as shown by the trend of the various mobile means obtained from the single measurements at a single point.

These diagrams confirm the presence of three or four distinct peaks that are subjected to a downward or upward shift caused by seasonal climatic changes and by infiltration of rainfall in the subsoil. A marked peak of S is always located immediately below the ground surface at a depth ranging from 20 cm to 50 cm. Secondary peaks can also be observed in the deeper colluvial layer at variable depths (120 and 150 cm), whereas the saturation degree considerably rises in proximity to the underlying weathered bedrock (Figure 10). The general shape of the saturation curves shows a sudden moisture increase at the base of the surficial organic soil, followed by a rapid decrease up to a depth of 50–100 cm. Below this minimum value, the saturation degree starts to increase again, reaching values close to 1 at depths greater than 200–250 cm.

The field observations obtained from the Dior colluvial slope have been confirmed by moisture data acquired from the Sedilis landslide. In the latter case, the saturation profile highlights a general curvilinear trend, with an exponential-shaped curve, showing an increase in the saturation degree as the depth increases, in particular for depths greater than 2.5–3.0 m (Figure 11). The saturation curve shows several localized peaks, analogously to the moisture profiles measured at the Dior slide. In this case, the mean value of the saturation degree is slightly higher (91%) than the Dior profiles (85%), and this depends on both the amount of precipitation which had previously fallen during the wet month of May (26 May 2020) and the larger content of clay fraction within the colluvium deposits (Tables 1 and 2). The saturation profile seems to indicate four separate peaks with abrupt variations in the deeper colluvial layer. The water content is particularly low in the top organic soil horizon, where a minimum value of $S = 72\%$ was recorded.

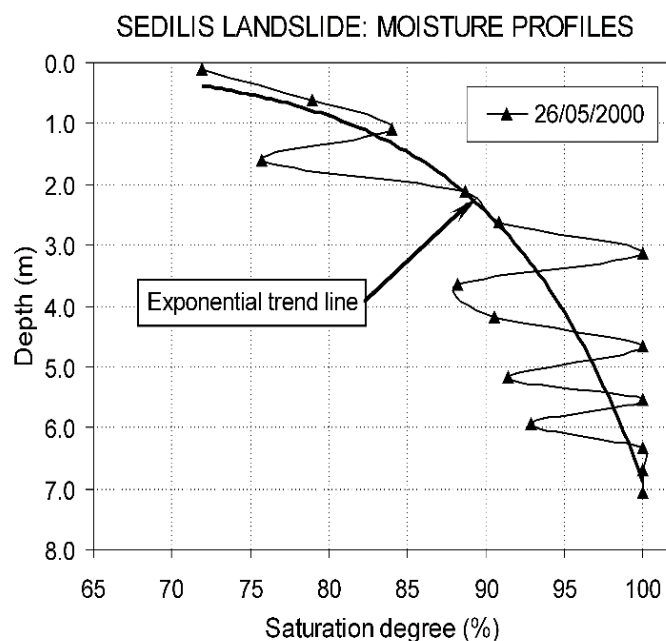


Figure 11. Saturation profiles recorded on 26 May 2000 on the colluvial slope involved in the Sedilis landslide (western lateral failure scarp). Note the four well-distinct maximum saturation peaks.

Saturation degree data, in addition to volumetric water content determinations, allow for useful considerations concerning the maximum void volume that can be filled by infiltrating rainfall. In the analyzed cases, the water fillable void volume varies from 0.15–0.20 m³ to 0.25–0.30 m³ for a reference area of 1 m² and a vertical column of thin cover (depth = 1–4 m) and thicker colluvium (depth = 4–8 m), respectively. These calculated water fillable volumes correspond with rainfall totals ranging from 150–300 mm, if we assume that rainfall totally infiltrates within the slope and surface water flows are neglected. As a consequence, complete saturation of colluvial slopes in northeastern Italy is a recurrent condition that is reached when the area is affected by storms with an intensity (*I*) greater than 150–200 mm for a 24-h duration, with a recurrence time (*Tr*) of about 5–10 years.

6. Soil–Water Characteristic Curves and Suction Profiles

In this work, some laboratory tests on selected soil samples were performed to obtain suction determinations that were necessary to reconstruct the SWCCs of the investigated colluvial slopes. These suction measurements were determined by following two different experimental methods: (1) by means of the pressure plate method for the Dior colluvial sediments [32]; and (2) by using a jet-fill tensiometer for the thicker colluvium of the Sedilis landslide. Both laboratory procedures allowed for the determination of suction experimental data related to a drying path characteristic curve.

6.1. Laboratory Tests

A specific laboratory procedure was performed and it was repeated for all samples taken from the colluvial slope to determine the SWCC for the Sedilis colluvium. Owing to the high percentage of gravel and pebbles within the colluvium (greater than 33–34%, as a rule), the finer fraction (diameter < 2 mm) was separated and then the soil samples were reconstituted into a state similar to that of the field conditions. The remolded samples were obtained using a finer soil matrix, i.e., only ASTM#40 sieve-passing material. They were prepared in a cylindrical steel mold with a total volume of 851 cm³ (diameter of 8.5 cm and height of 15 cm), with different controlled moisture and saturation degrees. After the initial phase of sample preparation and moisture adsorption, a jet-fill tensiometer (model 2725 by Soilmoisture Equipment Corporation, Santa Barbara, CA, USA, with water reservoir cap and refill mechanism) was inserted into a hole created within the soil sample for the suction measurement during the desorption stage. Suction measurements on this type of silty-loam reconstituted sample were performed after a stabilizing period of 24 h, which was required to achieve a good equilibrium condition. The measured suction values were corrected to take the height of the water in the tensiometer tube into account. Immediately afterwards, the suction measurement, volumetric water content θ_w and saturation degree *S* were determined on the tested soil samples. Based on this data, the reconstruction of the soil–water characteristic curve for low suction values, corresponding with the most frequent slope conditions, was possible. The results of the laboratory tensiometer tests are reported in Figure 12. Notably, these outcomes are consistent with previous determinations obtained from the Dior colluvial soils by Meriggi [32] using the pressure plate method and by the Fredlund and Xing [47] curves for silty soils. All the experimental data correspond with the field suction values characterizing the soils with an abundant silty fraction, and this is in accordance with the grain size properties of the investigated colluvial soils (Figure 8). It must also be noted that the occurrence of a considerable clay fraction in the investigated colluvial samples caused an increase in the suction values, as expected, with a shift of the measurement points of the characteristic curve towards the right (Figure 12). This explains how some experimental measurements fall near or beyond the drying curve for silty soils of Fredlund and Xing [47]. However, when considering the different test methods used to measure suction in the laboratory, the similarity of the general trend of experimental data is noteworthy.

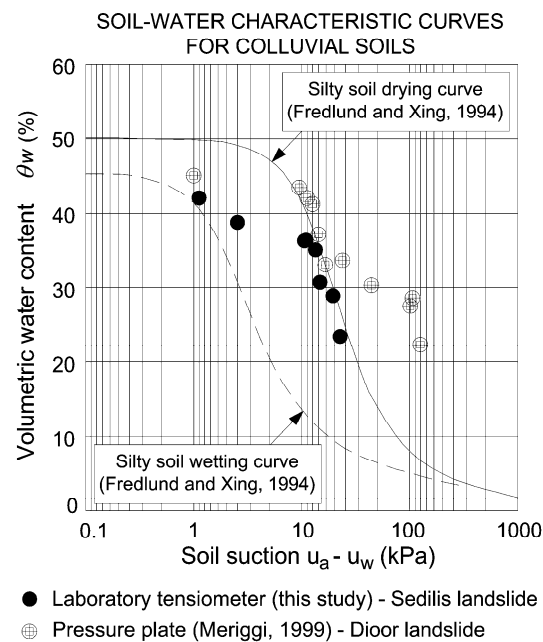


Figure 12. Experimental suction data ascertained from colluvium samples using both tensiometer and pressure plate measurement methods. For comparison purposes, wetting and drying soil–water characteristic curves for silty soils reported by Fredlund and Xing [47] are also shown.

6.2. Calculated Suction Profiles

The soil–water characteristic curve is the basic relationship necessary to describe and evaluate the hydrological and mechanical behavior of an unsaturated soil. This curve defines the relationship between suction and volumetric water content (θ_w). Suction is defined as a negative pore water pressure occurring within an unsaturated soil between the solid skeleton and the liquid phase. The matric suction is expressed by the difference between pore-air and pore-water pressure ($u_a - u_w$), and it can be defined as capillary pressure in the absence of an absorption phenomenon.

Many analytical expressions and equations of soil–water characteristic curves have been proposed by different authors in the past. Most formulations of the soil–water characteristic curves refer to a normalized volumetric water content [48–52]. In contrast, Williams et al. [53] and Fredlund and Xing [47] simply relate the soil–water characteristic curve with the volumetric water content θ_w defined as the ratio between the pore-water volume and the total volume (V_w/V_t). In this study, the equation proposed by Fredlund and Xing [47] was adopted, as follows:

$$\theta_w = C(\psi) \frac{\theta_s}{[\ln(e + (\psi/a)^n)]^m} \quad (1)$$

where:

e = natural number (i.e., 2.71828);

a = parameter related to the air entry value controlling the horizontal translation of the inclined branch of the characteristic curve;

n = exponent influencing the slope of the inclined branch;

m = exponent influencing the results near to the residual water content;

θ_s = volumetric water content for the whole saturated soil;

θ_w = volumetric water content;

ψ = suction at the volumetric water content θ_w ;

$C(\psi)$ = correction function depending on the residual water content. For low suction values, the correction function can be assumed as 1 [47].

The soil–water characteristic curves were determined by using the suction experimental measurements and the equation proposed by Fredlund and Xing [47], based on the parameters a , n and m . The calculated soil–water characteristic curves of the colluvial soils were finally adopted to reconstruct the variations of the inferred suction at depth, assuming the soil moisture profiles as reference cross sections. The purpose of this approach was to evaluate, for the analyzed case histories, the influence of low-spaced soil moisture determinations on the suction profiles, since in most cases only a few suction measurements (typically, three measuring points) were recorded in situ by means of tensiometer tests [27,29].

Two methods were employed to calculate the suction value existing at a given slope depth, and the results of these methods were then compared. Both methods utilized the experimental data obtained from the laboratory suction tests; that is, the tensiometer (Sedilis) and the pressure plate instrumentation (Dioor). On the basis of the experimental data points, the soil–water characteristic curve was determined and optimized within the analyzed range of low suction stress (<1500 kPa). The corresponding parameters were calculated according to Fredlund and Xing's [47] formulation (Dioor: $a = 65$, $n = 1.06$, $m = 1.09$; Sedilis: $a = 50$, $n = 1.25$, $m = 1.60$) (Figure 13).

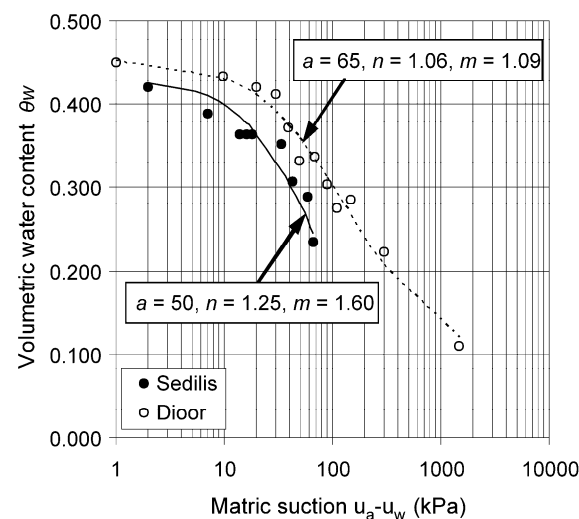


Figure 13. Soil–water characteristic curves related to the Dioor and Sedilis colluvial soils, using the equation suggested by Fredlund and Xing [47].

The first method is more rigorous and is based on the inversion of Fredlund and Xing's equation [47]. The equation is then solved in relation to θ_w , and the suction value ψ is obtained from the following relationship:

$$\psi = a \left[e^{(\theta_s/\theta_w)^{1/m}} - e \right]^{1/n} \quad (2)$$

This allows the calculation of suction values for both the laboratory samples and the field samples.

The second method is a best-fitting procedure of the experimental suction points. These points (ψ , θ_w) are inverted and best-fitted using a polynomial trend line to obtain the suction value ψ corresponding with the volumetric water content θ_w in the analyzed range (0–70 kPa).

The calculated suction profiles obtained for the Sedilis colluvial slope by using these two methods are compared in Figure 14, where both suction envelopes are very similar with just some small differences (0–12 kPa). The shape of the calculated suction profile (Figure 14) reproduces the general trend of the saturation curves already seen, but significant suction peaks are also identified and quantified. A maximum value of about 40–55 kPa characterizes the surficial soil layer, but a second suction peak (11–16 kPa) occurs at a greater depth (4–5 m) (Figure 14). The mean value of suction, calculated for the entire profile up to a depth of 7 m, is about 12 kPa and this is a value commonly quoted for loamy soils.

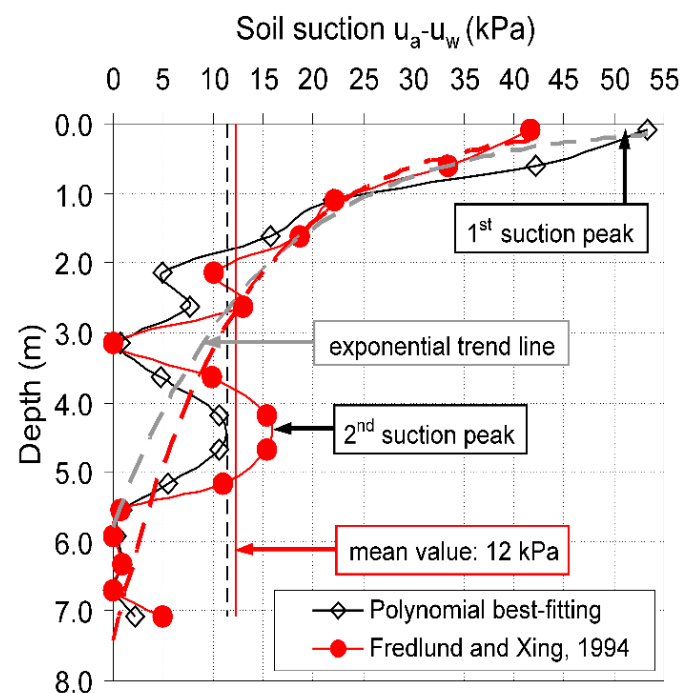


Figure 14. Comparison between calculated suction profiles for the Sedilis colluvial slope (western lateral scarp) that were obtained by inverting Fredlund and Xing's equation [47] and by means of a best-fitting procedure (polynomial trend line).

These calculation examples show that suction profiles in unsaturated colluvial slopes have a general trend that is more irregular than previously reported in case histories based on in situ tensiometer measurements. The added complexity of the actual slope stratigraphy can be recognized if the suction recording points are greater than those usually adopted at standard slope depths (0.5, 1.0, 1.5 m, for example). The comparison of in situ tensiometer data with calculated suction curves can improve knowledge about the suction variation within the slope, and localized laboratory information on soil samples can also be integrated using the data inferred by a simple slope moisture profile.

7. Conclusions

Infiltration and stability analyses of unsaturated colluvial slopes require an in-depth knowledge of the initial saturation condition of the slope. Although the water content is a well-known physical property that influences both the permeability and the shear strength of the soil, moisture profiles at depth are rarely reported in the literature. The analyzed case histories of unsaturated colluvial slopes of the alpine and pre-alpine areas of the Friuli Venezia Giulia Region demonstrate the importance of in situ soil moisture determinations before the infiltration models are carried out. For the two studied case histories (Dioir and Sedilis), the saturation degree (S) essentially varies from 65–70% (top layer or soil horizon) to the near-saturated basal colluvium ($S = 95$ –100%). This means that the colluvial cover is often close to the saturation condition, and values of the saturation degree lower than 50% have never been measured within the soil profile, even during the summer season. Average values of S , calculated for all the moisture profiles, range from 85–90%, and this is consistent with the very humid climate of the Friuli Venezia Giulia Region, where many areas are characterized by high values of cumulated yearly rainfall (1500–1800 mm/year, very often). Consequently, alpine colluvial slopes are in a near-saturated condition during most part of the year, particularly during the rainy months (September–November and May–June).

The average trend of the volumetric water content (θ_w) at depth (z) shows an exponential-shaped curve from the ground surface to the bottom layer, which corresponds well with suction profiles determined by in situ monitoring of residual slopes in Hong Kong [27]. However, the θ_w – z profiles are not gradual, and two or three marked saturation peaks can

occur. The occurrence of marked and repeated variations in the saturation degree reflects the stratigraphical complexity of the colluvial deposits, and this fact cannot be ignored in the infiltration analyses of the slope. Within the surficial soil horizons, the variation of θ_w at depth is strongly affected by pedogenetic features such as macro-porosity, root development, vertical fissures and clay illuviation. At a greater depth ($z > 1$ m), abrupt moisture variations in the colluvial slope are caused by marked lithostratigraphical changes due to complex sedimentary events that are very often related to previous slope failures provoking the remobilization of pre-existing landslide materials. For slopes characterized by repeated instability phenomena, this condition originates thick stratified colluvial deposits, which are particularly well developed within active or dormant landslide gullies (as the Sedilis landslide). For this reason, the shallow colluvial cover on terraced alluvial areas has to be differentiated from Flysch alpine relief, where diffuse concentrated water flows determine localized deep saturation conditions that can be recharged by a wide upslope drainage system (Sedilis). These site-specific conditions indicate that a detailed stratigraphical analysis of the colluvial deposits has to be performed before initiating the moisture profiling procedure in the field, in order to properly choose the sampling points. This is also true when planning selected points related to a field monitoring system designed for suction or water content measurements on a monitored slope.

In addition, the present work also shows that the water content profiling requires more suction measurement points than the three-point determinations that are usually reported (for example, $z = 0.5, 1.0$ and 1.5 m), as also demonstrated by Zhang et al. [28] for residual soils in China. In fact, the acquisition of excessive-spaced suction measurements along a slope profile characterized by closely stratified colluvial deposits may prevent the recognition of thin layers (thickness lower than 20–30 cm) that are in near-saturated conditions for most part of the year and that, consequently, have strong influence on the infiltration process related to the occurrence of heavy rainfall. In most cases, these near-saturated soil horizons contain a large amount of silt or clay fractions and, as a result, are characterized by lower shear strength properties. The combination of low shear resistance and high saturation degree makes these soil horizons prone to sliding, thus favoring the formation of a potential shear failure surface. This means that, when evaluating the stability condition of colluvial slopes, the unsuccessful identification of thin near-saturated layers can lead to an incorrect understanding of the slope stability problem. This work stresses the importance of performing a detailed lithostratigraphic analysis of the colluvial deposit in order to design a proper field measurement campaign and to correctly define the suction measurement points.

Moisture measurements based on multiple soil sampling in the field can be used to calculate the vertical variation of the soil matric suction if the soil–water characteristic curve is determined by employing some experimental procedures, both field and laboratory tests. This approach, based on laboratory suction measurements on colluvial samples, permitted the estimation of the suction profiles within the unsaturated slope by using the data obtained from the moisture profiling. Calculated suction profiles for the Dioor and Sedilis landslides indicate that maximum values ranging from 40 to 55 kPa often occur at the surficial soil slope (at depths lower than 0.2–0.5 m). This negative pore-water pressure greatly decreases after heavy rainfall events because of infiltration phenomena. Complete saturation of colluvial slopes in the alpine and pre-alpine regions of the Friuli Venezia Giulia Region generally requires rainfall that exceeds 150–200 mm for a 24-h storm duration. This results in a recurrence time of $Tr \cong 5$ –10 years for critical rainfall episodes hitting the Friulian colluvial slopes.

On the whole, this paper shows that water content and suction value assumptions in the infiltration models of colluvial slopes are often simpler than in real life. The in situ acquired moisture data demonstrates that colluvial slopes often exhibit a stratified structure, which implies the adoption of layered hydrological models. Input data for infiltration models and slope stability analyses must be strictly related to a detailed characterization of the colluvial slope, from both stratigraphical and hydrological points of view.

Author Contributions: Conceptualization, P.P., M.D.F. and A.B.; methodology, P.P., M.D.F. and A.B.; validation, P.P., M.D.F. and A.B.; formal analysis, P.P., M.D.F. and A.B.; investigation, P.P. and M.D.F.; resources, P.P., M.D.F. and A.B.; data curation, P.P., M.D.F. and A.B.; writing—original draft preparation, A.B.; writing—review and editing, P.P., M.D.F. and A.B.; visualization, A.B.; supervision, P.P., M.D.F. and A.B. All authors have read and agreed to the published version of the manuscript.

Funding: This research received no external funding.

Institutional Review Board Statement: Not applicable.

Informed Consent Statement: Not applicable.

Data Availability Statement: The data presented in this study are available within the article.

Conflicts of Interest: The authors declare no conflict of interest.

References

1. Kesseli, J.E. Disintegrating soil slips of the coast ranges of central California. *J. Geol.* **1943**, *51*, 342–352. [\[CrossRef\]](#)
2. Moser, M.; Hohensinn, F. Geotechnical aspects of soil slips in alpine regions. *Eng. Geol.* **1983**, *19*, 185–211. [\[CrossRef\]](#)
3. Varnes, D.J. Slope movement types and processes. In *Landslides: Analysis and Control, Special Report 176 National Research Council*; Schuster, R.L., Krizek, R.J., Eds.; TRB of the National Academy of Sciences: Washington, DC, USA, 1978; pp. 11–33.
4. Cruden, D.M.; Varnes, D.J. Landslide types and processes. In *Landslides: Investigation and Mitigation, Special Report 247 National Research Council*; Chapter 3; Turner, A.K., Schuster, R.L., Eds.; TRB of the National Academy of Sciences: Washington, DC, USA, 1996; pp. 36–75.
5. Johnson, K.A.; Sitar, N. Hydrologic conditions leading to debris-flow initiation. *Can. Geotech. J.* **1990**, *27*, 789–801. [\[CrossRef\]](#)
6. Pradel, D.; Raad, G. Effect of permeability on surficial stability of homogeneous slopes. *J. Geotech. Eng. ASCE* **1993**, *119*, 315–332. [\[CrossRef\]](#)
7. Anderson, S.A.; Sitar, N. Analysis of rainfall-induced debris flows. *J. Geotech. Eng. ASCE* **1995**, *121*, 544–552. [\[CrossRef\]](#)
8. Vanapalli, S.K.; Fredlund, D.G.; Pufahl, D.E.; Clifton, A.W. Model for the prediction of shear strength with respect to soil suction. *Can. Geotech. J.* **1996**, *33*, 379–392. [\[CrossRef\]](#)
9. Guzzetti, F.; Peruccacci, S.; Rossi, M.; Stark, C.P. Rainfall thresholds for the initiation of landslides in central and southern Europe. *Meteorol. Atmos. Phys.* **2007**, *98*, 239–267. [\[CrossRef\]](#)
10. Peranić, J.; Mihalić Arbanas, S.; Arbanas, Z. Importance of the unsaturated zone in landslide reactivation on flysch slope: Observations from Valići Landslide, Croatia. *Landslides* **2021**, *18*, 3737–3751. [\[CrossRef\]](#)
11. Tran, T.P.A.; Fredlund, D.G. Verification of the Fredlund (2019) Unsaturated Shear Strength Function. *Geosciences* **2021**, *11*, 151. [\[CrossRef\]](#)
12. Fredlund, D.G.; Morgenstern, N.R.; Widger, R.A. The shear strength of unsaturated soils. *Can. Geotech. J.* **1978**, *15*, 313–321. [\[CrossRef\]](#)
13. Fredlund, D.G.; Rahardjo, H. *Soil Mechanics for Unsaturated Soils*, 1st ed.; John Wiley & Sons, Inc.: New York, NY, USA, 1993; 517p.
14. Cavalcante, A.L.B.; Mascarenhas, P.V.S. Efficient approach in modeling the shear strength of unsaturated soil using soil water retention curve. *Acta Geotech.* **2021**, *16*, 3177–3186. [\[CrossRef\]](#)
15. Cho, S.E. Prediction of shallow landslide by surficial stability analysis considering rainfall infiltration. *Eng. Geol.* **2017**, *231*, 126–138. [\[CrossRef\]](#)
16. Yang, K.-H.; Uzuoka, R.; Thuo, J.N.; Lin, G.-L.; Nakai, Y. Coupled hydro-mechanical analysis of two unstable unsaturated slopes subject to rainfall infiltration. *Eng. Geol.* **2017**, *216*, 13–30. [\[CrossRef\]](#)
17. Zhang, J.; Zhu, D.; Zhang, S. Shallow slope stability evolution during rainwater infiltration considering soil cracking state. *Comput. Geotech.* **2020**, *117*, 103285. [\[CrossRef\]](#)
18. Cuomo, S.; Di Perna, A.; Martinelli, M. Modelling the spatio-temporal evolution of a rainfall-induced retrogressive landslide in an unsaturated slope. *Eng. Geol.* **2021**, *294*, 106371. [\[CrossRef\]](#)
19. Ng, C.W.W.; Shi, Q. A numerical investigation of the stability of unsaturated soil slopes subjected to transient seepage. *Comput. Geotech.* **1998**, *22*, 1–28. [\[CrossRef\]](#)
20. Dai, F.C.; Lee, C.F.; Sijing, W. Analysis of rainstorm-induced slide-debris flows on natural terrain of Lantau Island, Hong Kong. *Eng. Geol.* **1999**, *51*, 279–290.
21. Fourie, A.B.; Rowe, D.; Blight, G.E. The effect of infiltration on the stability of the slopes of a dry ash dump. *Géotechnique* **1999**, *49*, 1–13. [\[CrossRef\]](#)
22. Gasmo, J.M.; Rahardjo, H.; Leong, E.C. Infiltration effects on stability of a residual soil slope. *Comput. Geotech.* **2000**, *26*, 145–165. [\[CrossRef\]](#)
23. Cuomo, S.; Della Sala, M. Rainfall-induced infiltration, runoff and failure in steep unsaturated shallow soil deposits. *Eng. Geol.* **2013**, *162*, 118–127. [\[CrossRef\]](#)
24. Li, W.C.; Lee, L.M.; Cai, H.; Li, H.J.; Dai, F.C.; Wang, M.L. Combined roles of saturated permeability and rainfall characteristics on surficial failure of homogeneous soil slope. *Eng. Geol.* **2013**, *153*, 105–113. [\[CrossRef\]](#)

25. Morbidelli, R.; Corradini, C.; Saltalippi, C.; Flammini, A.; Dari, J.; Govindaraju, R.S. Rainfall infiltration modeling: A review. *Water* **2018**, *10*, 1873. [\[CrossRef\]](#)
26. Chiu, C.F.; Yan, W.M.; Yuen, K.-V. Reliability analysis of soil-water characteristics curve and its application to slope stability analysis. *Eng. Geol.* **2012**, *135–136*, 83–91. [\[CrossRef\]](#)
27. Lim, T.T.; Rahardjo, H.; Chang, M.F.; Fredlund, D.G. Effect of rainfall on matric suctions in a residual soil slope. *Can. Geotech. J.* **1996**, *33*, 618–628. [\[CrossRef\]](#)
28. Zhang, J.; Jiao, J.J.; Yang, J. In situ rainfall infiltration studies at a hillside in Hubei Province, China. *Eng. Geol.* **2000**, *57*, 31–38. [\[CrossRef\]](#)
29. Jeong, S.; Lee, K.; Kim, J.; Kim, Y. Analysis of rainfall-induced landslide on unsaturated soil slopes. *Sustainability* **2017**, *9*, 1280. [\[CrossRef\]](#)
30. Gui, M.-W.; Wu, Y.-M. Failure of soil under water infiltration condition. *Eng. Geol.* **2014**, *181*, 124–141. [\[CrossRef\]](#)
31. Bittelli, M.; Valentino, R.; Salvatorelli, F.; Rossi Pisa, P. Monitoring soil-water and displacement conditions leading to landslide occurrence in partially saturated clays. *Geomorphology* **2012**, *173–174*, 161–173. [\[CrossRef\]](#)
32. Meriggi, R. Misura delle proprietà idrauliche e meccaniche dei terreni colluviali in condizione di parziale saturazione. In Proceedings of the XX Convegno Nazionale di Geotecnica, AGI, Parma, Italy, 22–25 September 1999; pp. 177–184.
33. Peranić, J.; Arbanas, Z.; Cuomo, S.; Maček, M. Soil-water characteristic curve of residual soil from a Flysch rock mass. *Geofluids* **2018**, *2018*, 6297819. [\[CrossRef\]](#)
34. Jia, Y.-H.; Shao, M.-A.; Jia, X.-X. Spatial pattern of soil moisture and its temporal stability within profiles on a loessial slope in northwestern China. *J. Hydrol.* **2013**, *495*, 150–161. [\[CrossRef\]](#)
35. Li, T.; Shao, M.; Jia, Y.; Jia, X.; Huang, L. Profile distribution of soil moisture in the gully on the northern Loess Plateau, China. *Catena* **2018**, *171*, 460–468. [\[CrossRef\]](#)
36. Bordoni, M.; Meisina, C.; Valentino, R.; Lu, N.; Bittelli, M.; Chersich, S. Hydrological factors affecting rainfall-induced shallow landslides: From the field monitoring to a simplified slope stability analysis. *Eng. Geol.* **2015**, *193*, 19–37. [\[CrossRef\]](#)
37. Crawford, M.M.; Bryson, L.S.; Woolery, E.W.; Wang, Z. Long-term landslide monitoring using soil-water relationships and electrical data to estimate suction stress. *Eng. Geol.* **2019**, *251*, 146–157. [\[CrossRef\]](#)
38. Zhang, M.; Yang, L.; Ren, X.; Zhang, C.; Zhang, T.; Zhang, J.; Shi, X. Field model experiments to determine mechanisms of rainstorm-induced shallow landslides in the Feiyunjiang River basin, China. *Eng. Geol.* **2019**, *262*, 105348. [\[CrossRef\]](#)
39. Damiano, E.; Greco, R.; Guida, A.; Olivares, L.; Picarelli, L. Investigation on rainwater infiltration into layered shallow covers in pyroclastic soils and its effect on slope stability. *Eng. Geol.* **2017**, *220*, 208–218. [\[CrossRef\]](#)
40. Wang, F.; Dai, Z.; Takahashi, I.; Tanida, Y. Soil moisture response to water infiltration in a 1-D slope soil column model. *Eng. Geol.* **2020**, *267*, 105482. [\[CrossRef\]](#)
41. Wang, S.; Idinger, G.; Wu, W. Centrifuge modelling of rainfall-induced slope failure in variably saturated soil. *Acta Geotech.* **2021**, *16*, 2899–2916. [\[CrossRef\]](#)
42. Peranić, J.; Moscariello, M.; Cuomo, S.; Arbanas, Z. Hydro-mechanical properties of unsaturated residual soil from a flysch rock mass. *Eng. Geo.* **2020**, *269*, 105546. [\[CrossRef\]](#)
43. Fredlund, D.G. The 1999 R.M. Hardy Lecture: The implementation of unsaturated soil mechanics into geotechnical engineering. *Can. Geotech. J.* **2000**, *37*, 963–986. [\[CrossRef\]](#)
44. Paronuzzi, P.; Vanon, R. Eventi pluviometrici critici e dissesti: Studio della franosità del Comune di Paularo (Friuli—Alpi Carniche). *Geoling. Ambient. Min.* **1995**, *85*, 21–31.
45. Paronuzzi, P.; Cocco, A.; Garlatti, G. Eventi meteorici critici e debris flow nei bacini montani del Friuli. *L'Acqua* **1998**, *6*, 39–50.
46. Paronuzzi, P.; Del Fabbro, M.; Maddaleni, P. Frane superficiali su versanti alpini terrazzati della Val Chiarsò (Alpi Carniche—Friuli). *Geoling. Ambient. Min.* **2001**, *102*, 65–73.
47. Fredlund, D.G.; Xing, A. Equations for the soil-water characteristic curve. *Can. Geotech. J.* **1994**, *31*, 521–532. [\[CrossRef\]](#)
48. Gardner, W.R. Some steady-state solutions of the unsaturated moisture flow equation with application to evaporation from a water table. *Soil Sci.* **1958**, *85*, 228–232. [\[CrossRef\]](#)
49. Brooks, R.H.; Corey, A.T. Hydraulic properties of porous media. *Hydrol. Pap.* **1964**, *3*, 1–27.
50. van Genuchten, M.T. A closed-form equation for predicting the hydraulic conductivity of unsaturated soils. *Soil Sci. Soc. Am. J.* **1980**, *44*, 892–898. [\[CrossRef\]](#)
51. McKee, C.R.; Bumb, A.C. The importance of unsaturated flow parameters in designing a monitoring system for hazardous wastes and environmental emergencies. In Proceedings of the Hazardous Materials and Control Research Institute of Nature National Conference, Houston, TX, USA, 12–14 March 1984; pp. 50–58.
52. McKee, C.R.; Bumb, A.C. Flow-testing coalbed methane production wells in the presence of water and gas. *SPE Form. Eval.* **1987**, *2*, 599–608. [\[CrossRef\]](#)
53. Williams, J.; Prebble, R.E.; Williams, W.T.; Hignett, C.T. The influence of texture, structure and clay mineralogy on the soil moisture characteristic. *Aust. J. Soil Res.* **1983**, *21*, 15–32. [\[CrossRef\]](#)